Cancer Management and Research

Dovepress

open access to scientific and medical research

Open Access Full Text Article

ORIGINAL RESEARCH

Circular RNA circNHSL1 Contributes to Gastric Cancer Progression Through the miR-149-5p/YWHAZ Axis

This article was published in the following Dove Press journal:
Cancer Management and Research

Chunying Hui[1]
Lei Tian[1]
Xinling He[2]

[1]The Third Digestive Ward, The First Affiliated Hospital of Jinzhou Medical University, Jinzhou, Liaoning 121000, People's Republic of China; [2]Department of Hand and Foot Surgery, The First Affiliated Hospital of Jinzhou Medical University, Jinzhou, Liaoning 121000, People's Republic of China

Background: Gastric cancer (GC) is a considerable health burden around the world. Circular RNA Nance-Horan syndrome-like 1 (circNHSL1) is reported to be highly expressed in GC. Nevertheless, the function and molecule mechanism of circNHSL1 are still unclear.
Methods: The expression levels of circNHSL1, microRNA-149-5p (miR-149-5p) and YWHAZ were detected by real-time quantitative polymerase chain reaction (RT-qPCR). The subcellular fractionation identified the remarkable cytoplasmic localization of circNHSL1. Cell migration and invasion were measured by transwell assays. The levels of glutamine, glutamate and α-ketoglutarate (α-KG) were assessed by the corresponding kit. The protein levels of CD63, CD9, CD81, alanine, serine, cysteine-preferring transporter 2 (ASCT2), glutaminase 1 (GLS1), and tyrosine 3-monooxygenase/tryptophan 5-monooxygenase activation protein zeta (YWHAZ) were detected by Western blot assay. The binding relationship between miR-149-5p and circNHSL1 or YWHAZ was predicted by starBase 3.0 and then verified by RNA pull-down and dual-luciferase reporter assays. Xenograft tumor model examined the biological role of circNHSL1 in vivo. Exosomes were examined by a transmission electron microscope and nanoparticle tracking analysis (NTA).
Results: CircNHSL1 was highly expressed in GC cell-derived exosomes, GC tissues, and cells. Its knockdown impeded GC cell migration, invasion, and glutaminolysis. Mechanism analysis showed that circNHSL1 could affect YWHAZ expression by sponging miR-149-5p, thereby regulating GC progression. CircNHSL1 downregulation blocked GC tumor growth in vivo.
Conclusion: Our studies disclosed that circNHSL1 knockdown repressed migration, invasion, and glutaminolysis in vitro and inhibited tumor growth in vivo by miR-149-5p/YWHAZ axis in GC, implying an underlying circRNA-targeted therapy for GC treatment.
Keywords: circNHSL1, miR-149-5p, YWHAZ, gastric cancer

Introduction

As a common gastrointestinal malignancy, gastric cancer (GC) has become a considerable health burden socially, with approximately 780,000 deaths worldwide in 2018.[1] Although the surgical techniques and surgery have made an effective improvement, the prognosis of GC patients remains unfavorable due to the high recurrence rate and distant metastasis.[2] Moreover, since there are no specific symptoms at the initial phase, most people are often diagnosed at an advanced stage with extensive local invasion and migration.[3] Hence, it is necessary to identify a more effective biomarker and molecular mechanisms for elevating GC treatment.

Correspondence: Xinling He
Department of Hand and Foot Surgery, The First Affiliated Hospital of Jinzhou Medical University, No. 2, Section 5, Renmin Street, Jinzhou, Liaoning 121000, People's Republic of China
Tel +86-416-4197260
Email ticlbd@163.com

submit your manuscript | www.dovepress.com
DovePress
http://doi.org/10.2147/CMAR.S253152

Currently, circular RNAs (circRNAs), covalently linked to form a closed loop without 5′ caps or 3′ poly (A) tails, can regulate gene expression at the transcriptional or post-transcriptional level.[4] It was previously reported that circRNAs were widely expressed in exosomes and plasma, tissues and spatiotemporal specificity.[5,6] Moreover, with the development of sequencing technologies, circRNAs have attracted substantial attention due to their involvement in various diseases, including cancer.[7] Han et al reported that circRNA circ-BANP worked as competing endogenous RNA (ceRNA) to expedite lung cancer growth and metastasis by regulating LARP1 via miR-503.[8] Moreover, Zhu et al rendered that circRNA circ_0067934 could intensify hepatocellular carcinoma malignancy by boosting tumor growth, migration and invasion by sponging miR-1324 to impact FZD5 expression.[9] In a recent literature, it is suggested that derived from the Nance-Horan syndrome-like 1 (NHSL1) transcript, circNHSL1 (hsa_circ_0006835, chr6:-138794442–138817508), is a circRNA generated from two exons of NHSL1. It has been confirmed that circNHSL1 was upregulated in GC, and the dysregulation of circNHSL1 participates in the migration and invasion of GC.[10] Yet, the role and underlying mechanism of circNHSL1 in GC remain largely unknown.

During the past decades, microRNAs (miRNAs), a kind of conserved non-coding RNA (19–25 nucleotides), could bind to the 3′-untranslated region (3′UTR) of mRNAs to regulate the expression of target genes.[11] Previous publication has suggested that the abnormal expression of miRNAs is closely associated with the development and progression of diverse cancers, including GC.[12] MicroRNA-149-5p (miR-149-5p) is a form of mature of miR-149, which was reported as a tumor suppressor in multiple cancers, such as thyroid carcinoma,[13] cervical cancer,[14] and nasopharyngeal carcinoma.[15] Furthermore, some research has confirmed that miR-149 could repress the progression of GC by modulating target genes, like FOXM1,[16] ZBTB2,[17] and SP1.[18] These data indicated that miR-149 played a fatal role in the development of GC.

As a highly conservative protein in mammals, tyrosine 3-monooxygenase/tryptophan 5-monooxygenase activation protein zeta (YWHAZ) can mediate signal transduction through binding to phosphoserine-containing proteins.[19] Moreover, related studies have displayed that YWHAZ was upregulated in a variety of tumors, and contributed to tumor progression.[20,21] Notably, YWHAZ was reported to be increased in GC and served as a co-carcinogenic factor by inducing proliferation and metastasis in GC development,[22,23] suggesting the important function of YWHAZ in GC.

Here, our data exhibited that circNHSL1 was upregulated in GC cell-derived exosomes, GC tissues and cells. Functionally, circNHSL1 silencing hindered migration, invasion, and glutaminolysis of GC cells. Bioinformatics analysis discovered that miR-149-5p was a direct target of circNHSL1 in GC cells. Thus, we aimed to explore whether circNHSL1 could exert the function through regulating the miR-149-5p/YWHAZ axis in GC progression.

Materials and Methods

Clinical Samples and Cell Culture

Samples of serum and tissues from GC patient (n=20) and healthy volunteers (n=20) were collected from The First Affiliated Hospital of Jinzhou Medical University. In this research, we obtained the approval of the Ethics Committee of The First Affiliated Hospital of Jinzhou Medical University, and every participant signed the written informed consent. The clinical information of the patients included age, gender, tumor size, TNM stage, lymphatic metastasis, and distant metastasis is summarized in Table 1.

Human GC cell lines (HGC-27 and AGS) were provided by Cell Bank of the Chinese Academy of Sciences (Shanghai, China).The Human normal gastric epithelial cell line (GES-1) was acquired by the Beijing Institute of Cancer Research (Beijing, China). All cells were cultured in 5% CO_2 at 37°Cunder moist atmosphere with Roswell Park Memorial Institute medium 1640 (RPMI-1640; PAN-Biotech GmbH, Aidenbach, Germany). Noteworthily, supplemented culture medium displayed a medium with 10% fetal bovine serum (FBS; Gibco, Grand Island, NY, USA) and 1% penicillin/streptomycin (KeyGen, Nanjing, China).

Real-Time Quantitative Polymerase Chain Reaction (RT-qPCR)

Total RNA from each sample was extracted, referring to the supplier's direction TRIzol (TaKaRa, Dalian, China).[24] The extracted RNA concentration was quantified using NanoDrop (NanoDrop Technologies, Wilmington, WI, USA). Subsequently, these RNAs were reversely transcribed into the first-strand complementary DNA (cDNA) by using the PrimeScript RT Master Mix Reagent (TaKaRa).And RT-qPCR was executed on a LightCycler® 480 (Roche diagnostics, Mannheim, Germany) with an SYBR Green PCR kit (Takara). With the help of $2^{-\Delta\Delta Ct}$

Table 1 Correlation Between circNHSL1 Expression and Clinical Clinicopathological Parameters of GC

Parameter	Case	circNHSL1 Expression		*P* value[a]
		Low (n=11)	High (n=9)	
Age (years)				0.279
≤60	7	5	2	
>60	13	6	7	
Gender				0.714
Female	12	7	5	
Male	8	4	4	
Tumor size				0.006*
≤5 cm	11	3	8	
>5 cm	9	8	1	
TNM stages				0.02*
I–II	10	8	2	
III–IV	10	3	7	
Lymphatic metastasis				0.04*
Negative	13	5	8	
Positive	7	6	1	
Vascular invasion				0.582
Absent	8	5	3	
Present	12	6	6	
Distant metastasis				0.02*
M_0	14	10	4	
M_1	6	1	5	

Note: *$P < 0.05$; [a]Chi-square test.
Abbreviations: GC, gastric cancer; TNM, tumor-node-metastasis.

method,[25] the data were normalized with glyceraldehyde-3-phosphate dehydrogenase (GAPDH for circNHSL1, NHSL1, and YWHAZ) and U6 small nuclear RNA (snRNA for miR-149-5p). The primer sequences were exhibited as follows:

circNHSL1: 5′-AGCTAGGACTACAGTCTTTCCAGTGGAATGGA-3′ (sense), 5′-TCTGTCCGTTTACTATTG-3′ (antisense);

NHSL1: 5′-AGCAGAGTGGAAGCCAATGTC-3′ (sense), 5′-ACCTCATCATTCCCGTCTTCC-3′ (antisense);

miR-149-5p: 5′-TCTGGCTCCGTGTCTTCACTCCC-3′ (sense), the common reverse primer sequence was provided by the SYBR Green PCR kit;

YWHAZ: 5′-TTTCTCCTTCCCCTTCTTCCG-3′ (sense), 5′-TTTCTCCTTCCCCTTCTTCCG-3′ (antisense);

U6: 5′-CTCGCTTCGGCAGCACA-3′ (sense), 5′-AACGCTTCACGAATTTGCGT-3′ (antisense);

GAPDH: 5′-GTCAACGGATTTGGTCTGTATT-3′ (sense), 5′-AGTCTTCTGGGTGGCAGTGAT-3′ (antisense).

Cell Transfection

For the YWHAZ overexpression vector, the full sequence of YWHAZ was introduced into pcDNA3.1 empty vector (pc, Invitrogen, Waltham, MA, USA), named as pc-YWHAZ, and pcDNA3.1 empty vector acted as a negative control (pc-NC). CircNHSL1 small interfering RNA (si-circNHSL1) and its negative control (si-NC), miR-149-5p mimic, miR-149-5p inhibitor and their negative controls (miRNA NC and inhibitor NC) were obtained from GenePharma (Shanghai, China). According to the manufacturer's instructions, Lipofectamine 3000 reagent (Invitrogen) was applied for transfection.

RNase R Treatment and Subcellular Fractionation Assay

For RNase R treatment, total RNA was incubated with or without RNase R (3 U/mg, Epicentre, Shanghai, China) at 37°C for 15 min, followed by the purification with phenol-chloroform (Sigma-Aldrich, St. Louis, MO, USA). And then, RT-qPCR assay was performed to detect the levels of circNHSL1 and NHSL1.

For subcellular fractionation assay, HGC-27 and AGS cells were suspended and centrifuged in cytoplasm lysis buffer. After collecting the cytoplasmic supernatant, the rest was incubated and centrifuged in nucleus lysis buffer. Whereafter, TRIzol reagent (TaKaRa) was used for the extraction of RNAs from cytoplasmic and nuclear. At last, the levels of circNHSL1, U6 (nucleus control), and GAPDH (cytoplasm control) were measured by RT-qPCR assay in cytoplasmic and nuclear.

Transwell Assay

The capacities of migration and invasion in HGC-27 and AGS cells were assessed based on the user's guidebook of the transwell chamber (Chemicon, Temecula, CA, USA). Notably, for invasion assay, the transwell chamber was pre-coated with Matrigel (BD Biosciences, San Jose, CA, USA). Briefly, GC cells (1×10^5) in serum-free culture medium were added to the upper chamber, and the lower chamber was filled with the medium containing 10% FBS (Gibco, as chemoattractant). The cells remaining in the upper chambers were removed after incubation for 24 h, and the cells on the lower surface were fixed and stained

with 0.1% crystal violet. Finally, a microscope (Tecan, Switzerland) was applied for the migrated or invaded cells.

Measurement of Glutamine, Glutamate, and α-KG Levels

In this assay, the levels of glutamine, glutamate, and α-ketoglutarate (α-KG) in HGC-27 and AGS cells were analyzed in accordance with the instructions of Glutamine Determination Kit (BioVision, Milpitas, CA, USA), Glutamate Determination Kit (BioVision) and α-KG Assay Kit (Abcam).

Western Blot Assay

Briefly, protein lysates from the samples were harvested in line with the operation manual of RIPA buffer with protease and phosphates inhibitions (Beyotime, Shanghai, China), followed by the quantification with a BCA Protein Assay Kit (Beyotime). Then, a sodium dodecyl sulfate-polyacrylamide gel electrophoresis (SDS-PAGE) system was applied to separate the extracted proteins, which were then transferred onto nitrocellulose membranes (Millipore Corp, Bedford, MA, USA), followed by blockage with 5% skim milk for 2 h. After incubation at 4°C overnight with primary antibodies against CD63 (1:1000, ab68418, Abcam, Cambridge, MA, USA), CD9 (1:1000, ab92726, Abcam), CD81 (1:1000, ab155760, Abcam), Alanine, serine, cysteine-preferring transporter 2 (ASCT2; 1:1000, ab84903, Abcam), glutaminase 1 (GLS1; 1:1000, ab93434, Abcam), YWHAZ (1:1000, ab51129, Abcam) and GADPH (1:1000, ab8227, Abcam), the membranes were treated with the corresponding horseradish peroxidase (HRP)-conjugated secondary antibodies for 2 h. Finally, the bands were analyzed according to the manufacturer's instructions of enhanced chemiluminescence reagent (ECL, Pierce Biotechnology, Rockford, IL, USA).

RNA Pull-Down Assay

For the biotin-coupled probe pull-down assay, the biotinylated-circNHSL1 probe was specifically designed and synthesized through GenePharma (Shanghai, China), and oligo probe acted as a control. In brief, GC cells (1×10^7) in lysis buffer were incubated with the designed probes for 2 h. Then, the biotin-coupled RNA complex was pull-downed by incubating the GC cell lysates with M-280 Streptavidin magnetic beads (Invitrogen). At 4 h post-incubation, the beads were washed with lysis buffer, and the RNA complexes bound to the beads were extracted with Trizol reagent (TaKaRa) and analyzed by RT-qPCR assay.

For biotin-coupled miRNA capture, GC cells (5×10^6) were transfected with biotinylated miR-149-5p mimic (biotin-miR-149-5p, GenePharma) or nonsense control (biotin-NC, GenePharma) based on the user's guidebook of Lipofectamine RNAiMax (Invitrogen). At 48 h after transfection, M-280 Streptavidin magnetic beads (Invitrogen) were washed with lysis buffer, followed by blockage with yeast tRNA on the rotator at a low speed (10r/min). After lysis and ultrasonic treatment, GC cells were incubated with the blocked beads at 4°C. The next day, Trizol reagent (TaKaRa) was used to purify bound RNAs, and RT-qPCR assay was conducted to assess the abundance of circNHSL1 in bound fractions.

Dual-Luciferase Reporter Assay

To construct circNHSL1 wild type (WT), circNHSL1 mutant type (MUT), WT-YWHAZ-3′-untranslated region (3′UTR) and MUT-YWHAZ-3′UTR reporters, the sequences of circNHSL1 and the 3′UTR of YWHAZ containing putative binding sites of wild-type miR-149-5 or mutated miR-149-5 were amplified and inserted into the psiCHECK vector (Promega, Fitchburg, WI, USA). With the help of Lipofectamine 3000 (Invitrogen), GC cells were co-transfected with circNHSL1 WT/MUT or YWHAZ WT/MUT and miR-149-5 mimics or miRNA-NC, followed by incubation for 48 h. At last, a dual-luciferase reporter assay system (Promega) was utilized to analyze the luciferase activities.

Tumor Xenograft Assay

Lentiviral-based short hairpin RNA (shRNA) targeting circNHSL1 (sh-circNHSL1) and the lentivirus empty vector as a control (sh-NC) were provided by GeneChem (Shanghai, China). The animal experiment was approved by the Animal Ethics Committee of The First Affiliated Hospital of Jinzhou Medical University. Animal studies were performed in compliance with the ARRIVE guidelines and the Basel Declaration. All animals received humane care according to the National Institutes of Health (USA) guidelines. Male BALB/C nude mice were provided by the National Laboratory Animal Center (Beijing, China) and divided into 2 groups (n=8 per group). HGC-27 cells (5×10^6) with sh-circNHSL1 or sh-NC were subcutaneously injected in the left flank of the nude mice. At 7 days after injection, tumor volume was detected every 4 days. Twenty-seven days later, tumors

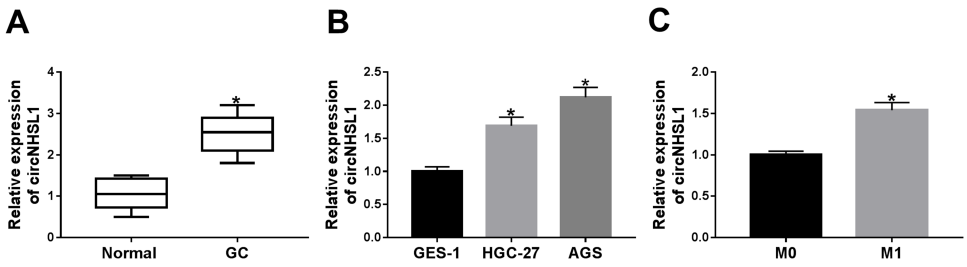

Figure 1 CircNHSL1 was increased in GC tissues and cells. (**A**) CircNHSL1 level was detected in 20 pairs of GC tissues and matched normal controls. (**B**) The expression level of circNHSL1 was tested in human normal gastric epithelial cell line (GES-1) and GC cell lines (HGC-27 and AGS). (**C**) CircNHSL1 level was measured in M0 stage and M1 stage of GC tissues. *P <0.05.

were excised and weighed, followed by utilization for RT-qPCR assay and Western blot assay.

Exosome Detection

Exosomes were extracted from serums and cells by using ultracentrifugation and total exosome isolation kit (Invitrogen) as per the instruction guidelines. A transmission electron microscope was applied to examine the extracted exosomes according to the previously described.[26] In the nanoparticle tracking analysis (NTA), a Nanosight NS300 system (Nanosight, Amesbury, UK) was used to track the number and size of exosomes, and the system was configured a high-sensitivity camera and a laser light source (488 nm).

Statistical Analysis

GraphPad Prism7 software was applied to conduct the statistical analysis. Comparison of two or more groups was evaluated by using Student's *t*-test or one-way analysis of variance (ANOVA) with Tukey's tests. Pearson correlation analysis was used to analyze the expression association.Data were displayed as mean ± standard deviation (SD). If P value < 0.05, it was considered as statistically significant.

Results

CircNHSL1 Was Increased in GC Tissues and Cells

Firstly, we examined the expression level of circNHSL1 in 20 pairs of GC tissues and matched normal controls. As displayed in Figure 1A, the marked upregulation of circNHSL1 was viewed in the GC sample. Consistent with the results of GC tissues, circNHSL1 expression was higher in GC cell lines (HGC-27 and AGS) than in the human normal gastric epithelial cell line (GES-1) (Figure 1B).Then, we divided the patients into two groups (High and Low) using the median value of circNHSL1 expression levels in GC patients. As presented in Table 1, our results indicated that the high circNHSL1 expression was significantly associated with Tumor size (p=0.006), TNM stages (p=0.02), lymphatic metastasis (p=0.04), and Distant metastasis (p=0.02). However, there was no correlation between circNHSL1 expression and other clinical parameters. Moreover, our data also confirmed that circNHSL1 was highly expressed in tissues with the M1 stage compared with the M0 stage (Figure 1C), suggesting the oncogenic factor of circNHSL1 in GC. In a word, these data suggested the involvement of circNHSL1 in the progression of GC.

CircNHSL1 Deficiency Suppressed Migration, Invasion, and Glutaminolysis of GC Cells

Furthermore, to identify the stability of circNHSL1, HGC-27 and AGS cells were treated with RNase R. As presented in Figure 2A and B, the treatment of RNase R strikingly reduced the mRNA level of NHSL1, while had little effect on circNHSL1 level, indicating that circNHSL1 was a circular RNA. Synchronously, nuclear and cytoplasmic separation assays further verified that circNHSL1 was predominantly localized in the cytoplasm of HGC-27 and AGS cells (Figure 2C and D), suggesting the underlying post-transcriptional regulatory mechanism of circNHSL1 in GC cells. Besides, considering the high expression of circNHSL1 in GC, thus, we knocked down circNHSL1 in HGC-27 and AGS cells. Results showed that the transfection of si-circNHSL1 hindered the expression level of circNHSL1 but had no apparent effect on the NHSL1 mRNA level (Figure 2E), implying that knockdown only worked on the circular RNA. Functionally, the deletion of circNHSL1 notably repressed migration (Figure 2F and G) and invasion (Figure 2H and I) of HGC-27 and AGS cells. Besides,

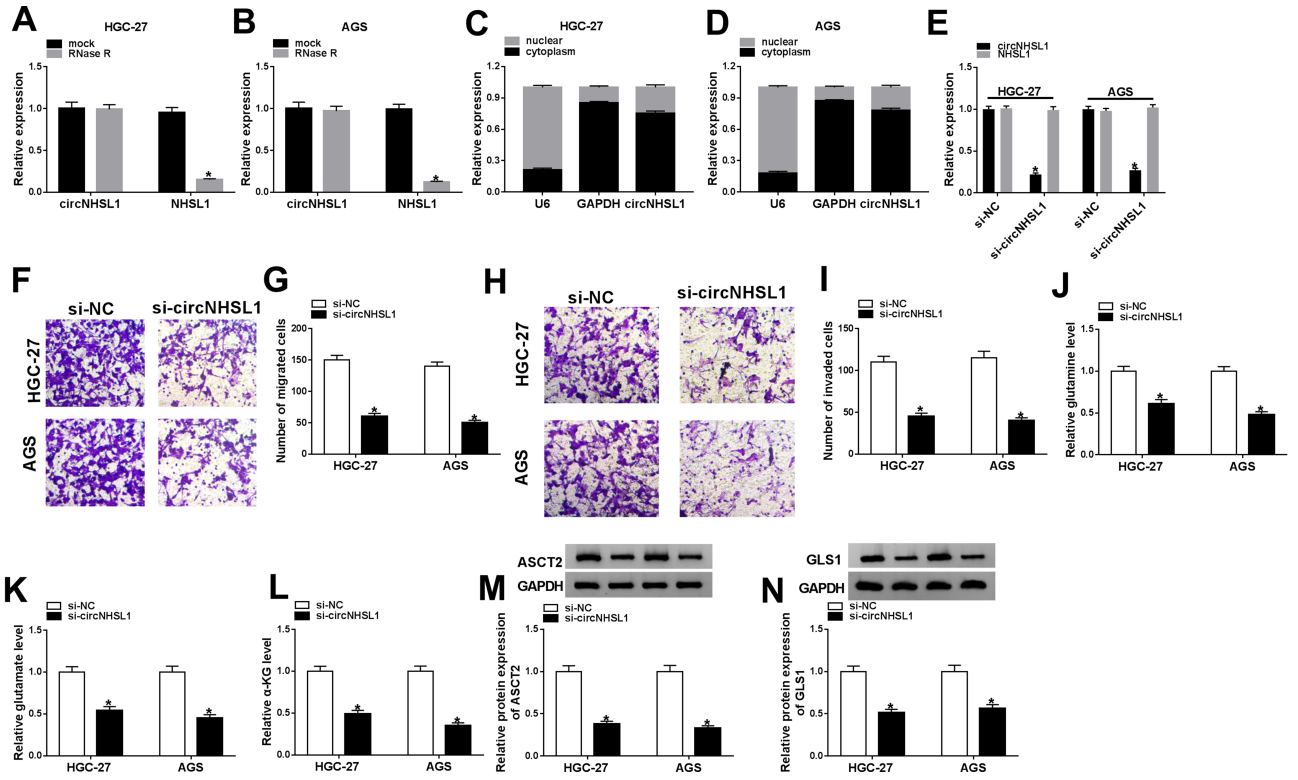

Figure 2 CircNHSL1 knockdown inhibited migration, invasion and glutaminolysis of GC cells. (**A** and **B**) Relative levels of circNHSL1 and NHSL1 mRNA were tested in HGC-27 and AGS cells treated with or without RNase R. (**C** and **D**) The cellular localization of circNHSL1 in HGC-27 and AGS cells was analyzed by Subcellular fractionation. (**E**) The levels of circNHSL1 and NHSL1were detected in HGC-27 and AGS cells transfected with si-NC and si-circNHSL1. (**F** and **G**) Transwell migration assay was carried out to measure the capacity of migration in transfected HGC-27 and AGS cells. (**H** and **I**) Transwell invasion assay was applied to assess the ability of invasion in transfected HGC-27 and AGS cells. (**J–L**) Relative levels of glutamine, glutamate and α-KG were assessed in transfected HGC-27 and AGS cells. (**M** and **N**) Protein levels of ASCT2 and GLS1 were examined in transfected HGC-27 and AGS cells. *P <0.05.

glutaminolysis has been reported as a marker of metabolic recombination in cancer.[27] Meanwhile, the survival and proliferation of cancer cells are highly dependent on glutamine, and ASCT2, a high-affinity glutamine importer, is involved in the accelerated uptake of glutamine.[28] However, with the help of a rate-limiting enzyme GLS1, glutamine is converted to glutamate, which is then transformed into α-KG.[29] Therefore, we further explored the impact of circNHSL1 on glutaminolysis in GC cells. First of all, we measured the expression levels of glutaminolysis metabolites in GC cells. As shown in Figure 2J-L, the decreased expression of glutamine, glutamate, and α-KG was observed caused by the downregulation of circNHSL1. Simultaneously, we further examined the levels of glutamine importer ASCT2 and the glutaminolysis pathway-associated rate-limiting enzyme GLS1. Similarly, in HGC-27 and AGS cells, Western blot results indicated that the protein levels of ASCT2 and GLS1 were suppressed due to the knockdown of circNHSL1 (Figure 2M and N). Collectively, these results suggested that the silencing of circNHSL1 could block migration, invasion, and glutaminolysis of GC cells.

CircNHSL1 Targeted miR-149-5p

It has been confirmed that circRNAs could exert the role by interacting with miRNAs.[30] Through bioinformatics softwarestarBase3.0, we found that miR-149-5p contained some complementary sequences with circNHSL1 (Figure 3A). To identify the underlying miRNA, a 3′-terminal-biotinylated-circNHSL1 probe was designed. As displayed in Figure 3B, miR-149-5p was abundantly polled down by the circNHSL1 probe in HGC-27 and AGS cells. Then, to confirm the direct binding of circNHSL1 and miR-149-5p, biotin-labeled miR-149-5p and biotin-NC (as a negative control) were designed to pull down circNHSL1 in HGC-27 and AGS cells. Results suggested that miR-149-5p captured more circNHSL1 relative to the control group (Figure 3C). Consistent with bioinformatics analysis results and RNA pull-down assay, dual-luciferase reporter assay proved that the upregulation of miR-149-5p declined the luciferase activity of circNHSL1 WT, whereas had no effect on the luciferase activity of circNHSL1 MUT reporter vector in HGC-27 and AGS cells (Figure 3D and E). Meanwhile, we found that

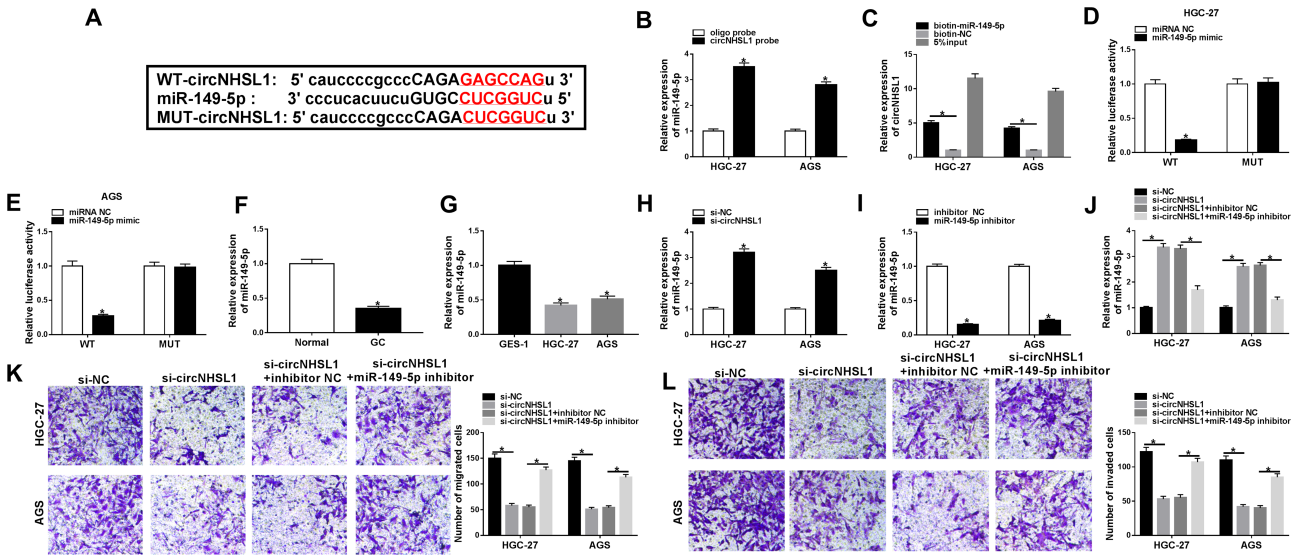

Figure 3 MiR-149-5p was a direct target of circNHSL1. (**A**) The binding sites between circNHSL1 and miR-149-5p were predicted by starbase3.0 software. (**B**) MiR-149-5p level was detected in lysates of HGC-27 and AGS cells treated with oligo probe or circNHSL1 probe. (**C**) RNA pull-down assay was performed in HGC-27 and AGS cells extracts to verify that circNHSL1 could directly bind to miR-149-5p. (**D** and **E**) Dual-luciferase reporter assay was preformed to confirm the binding relationship between circNHSL1 and miR-149-5pin HGC-27 and AGS cells. (**F**) MiR-149-5p level was tested in 20 pairs of GC tissues and paired normal controls. (**G**) Relative expression of miR-149-5p was detected in GES-1, HGC-27 and AGS cells. (**H**) MiR-149-5p level was assessed in HGC-27 and AGS cells transfected with si-NC and si-circNHSL1. (**I**) MiR-149-5p level was examined in HGC-27 and AGS cells transfected with inhibitor NC and miR-149-5p inhibitor. (**J**) Relative expression of miR-149-5p was detected in HGC-27 and AGS cells treated with si-NC, si-circNHSL1, si-circNHSL1 + inhibitor NC and si-circNHSL1 + miR-149-5p inhibitor. (**K** and **L**) Migration and invasion were analyzed in treated HGC-27 and AGS cells. *P <0.05.

miR-149-5p expressed at the low level in GC tissues and cells compared to respective control groups (Figure 3F and G), and was negatively correlated tocircNHSL1 expression (Figure S1). And the miR-149-5p level was distinctly impeded in si-circNHSL1-transfected HGC-27 and AGS cells with respect to cells with si-NC (Figure 3H). To further explore the function of miR-149-5p in GC cells, we knocked down the expression level of miR-149-5p in HGC-27 and AGS cells. And the transfection efficiency of miR-149-5p inhibitor was measured and shown in Figure 3I. Rescue assay proved that circNHSL1 deletion promoted the expression level of miR-149-5p, while the re-introduction of miR-149-5p inhibitor abated the effect (Figure 3J). Functional analysis confirmed that miR-149-5p downregulation drastically mitigated the inhibitory effect of circNHSL1 knockdown on migration and invasion in HGC-27 and AGS cells (Figure 3K and L). These data discovered that miR-149-5p, as a target of circNHSL1, partially abolished the effect of circNHSL1 on migration and invasion in GC cells.

CircNHSL1 Knockdown Repressed Glutaminolysis by Regulating miR-149-5p in GC Cells

As mentioned above, circNHSL1 played a crucial role in the glutaminolysis of GC cells. Furthermore, miR-149-5p was a direct target of circNHSL1 in GC cells. Therefore, we further explored whether circNHSL1 could regulate glutaminolysis by interacting with miR-149-5p inHGC-27 and AGS cells. As exhibited in Figure 4A-C, the deficiency of miR-149-5p partly abolished circNHSL1 knockdown-caused reduction in glutamine, glutamate, and α-KG in HGC-27 and AGS cells. Consistently, the suppression of ASCT2 and GLS1 triggered by si-circNHSL1 was reversed through the silencing of miR-149-5p in HGC-27 and AGS cells (Figure 4D-F).In a word, circNHSL1 deletion could constrain the glutaminolysis of GC cells through modulating miR-149-5p.

YWHAZ Was a Target of miR-149-5p

To further explore the regulatory mechanism of miR-149-5p in GC cells, we searched the latent target mRNA of miR-149-5p by bioinformatics software Starbase3.0. As displayed in Figure 5A, YWHAZ-3′UTR was found to possess some complementary sites with miR-149-5p. Whereafter, a dual-luciferase reporter assay was conducted to verify the predicted results. Data suggested that miR-149-5p mimic strikingly reduced the luciferase activity of WT-YWHAZ -3′UTR reporter but not that of MUT-YWHAZ-3′UTR reporter (Figure 5B and C). Meanwhile, the miR-149-5p level was upregulated in miR-149-5p mimic-transfected HGC-27 and AGS cells relative to cells with miR-NC (Figure 5D).

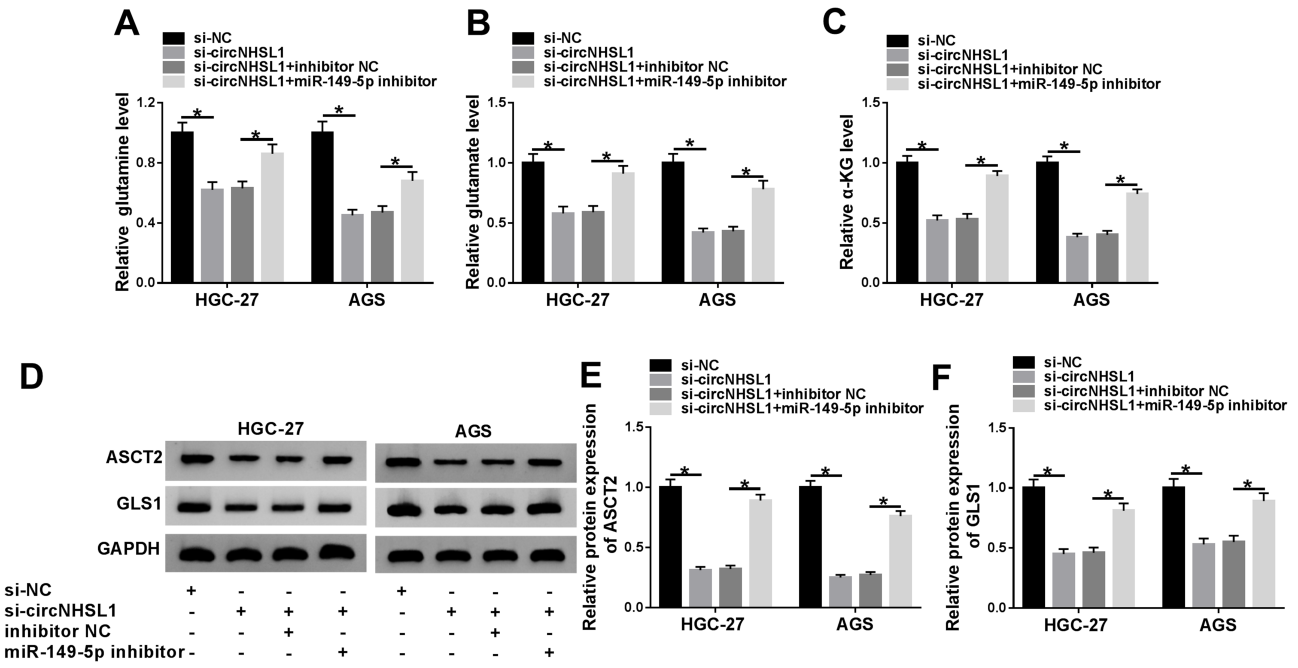

Figure 4 MiR-149-5p silencing abrogated the effects of circNHSL1 knockdown on glutaminolysis in GC cells. (**A–C**) The levels of glutamine, glutamate and α-KG were detected in HGC-27 and AGS cells transfected with si-NC, si-circNHSL1 and si-circNHSL1 + inhibitor NC and si-circNHSL1 + miR-149-5p inhibitor. (**D–F**) Protein levels of ASCT2 and GLS1 were tested in transfected HGC-27 and AGS cells. *P <0.05.

Interestingly, the overexpression of miR-149-5p hindered the mRNA level and protein level of YWHAZ in HGC-27 and AGS cells (Figure 5E and F). To further explore the role of YWHAZ in GC, we used the Cancer Genome Atlas (TCGA) database to examine the expression of YWHAZ in stomach adenocarcinoma (STAD). As a result, YWHAZ expression was high in primary tumor and individual cancer stages in comparison with respective controls (Figure S2). Moreover, Western blot results confirmed that the YWHAZ level was increased in GC tissues and cells when compared with their respective control groups (Figure 5G and H), and was inversely associated with miR-149-5p expression in GC tissues (Figure S1). To identify the function of YWHAZ in GC cells, we over-expressed YWHAZ in HGC-27 and AGS cells. As shown in Figure 5I and J, the YWHAZ level was strikingly upregulated in pc-YWHAZ-transfected HGC-27 and AGS cells versus cells transfected with pc-NC. Importantly, YWHAZ overexpression prominently abrogated the negative influence of miR-149-5p upregulation on the level of YWHAZ in HGC-27 and AGS cells (Figure 5K and L). Apart from that, the functional analysis suggested that the abilities of migration and invasion repressed by miR-149-5p mimic were markedly overturned through the re-introduction of pc-YWHAZ in HGC-27 and AGS cells (Figure 5M and N).Overall, these results suggested that miR-149-5p could regulate migration and invasion of GC cells by targeting YWHAZ.

YWHAZ Overexpression Reversed miR-149-5p-Mediated Glutaminolysis in GC Cells

Next, we further explored the regulatory function of miR-149-5p and YWHAZ in the glutaminolysis of HGC-27 and AGS cells. As exhibited in Figure 6A-C, miR-149-5p overexpression led to an overt reduction in the levels of glutamine, glutamate, and α-KG in HGC-27 and AGS cells, which was abrogated by the upregulation of YWHAZ. Similarly, pc-YWHAZ partly overturned miR-149-5p mimic-triggered decline in ASCT2 and GLS1 protein levels in HGC-27 and AGS cells (Figure 6D-F). Taken together, miR-149-5p could inhibit glutaminolysis by regulating YWHAZ in GC cells.

Verification of circNHSL1/miR-149-5p/YWHAZ Regulatory Axis in GC Cells

Based on the above results, we speculated that circNHSL1 could exert its function by regulating the miR-149-5p/YWHAZ axis. Hence, we examined the effect of circNHSL1 on YWHAZ expression in GC cells. CircNHSL1 deletion curbed the level of YWHAZ in HGC-27 and AGS cells,

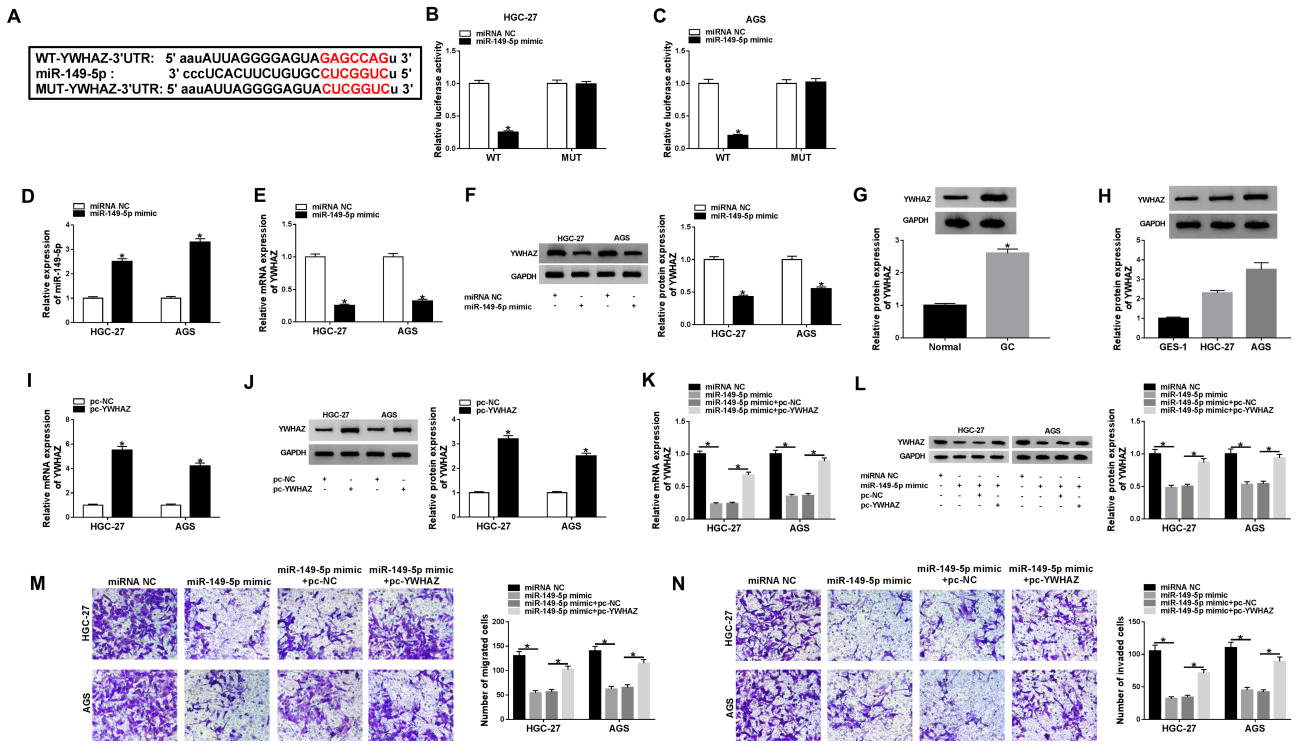

Figure 5 YWHAZ acted as the target of miR-149-5p. (**A**) Starbase3.0 software was conducted to predict the binding sequences between miR-149-5p and YWHAZ-3'UTR. (**B** and **C**) The effects of miR-149-5p overexpression on luciferase activity of WT-YWHAZ and MUT-YWHAZ reporters in HGC-27 and AGS cells were measured by a dual-luciferase reporter assay. (**D**) MiR-149-5p level was detected in HGC-27 and AGS cells transfected with miR-NC and miR-149-5p mimic. (**E** and **F**) YWHAZ level was measured in HGC-27 and AGS cells transfected with miR-NC and miR-149-5p mimic. (**G** and **H**) YWHAZ protein level was detected in GC tissues, GC cell lines (HGC-27 and AGS cells) and respective control groups. (**I** and **J**) YWHAZ level was measured in HGC-27 and AGS cells transfected with pc-NC and pc-YWHAZ. (**K** and **L**) YWHAZ level was detected in HGC-27 and AGS cells treated with miR-NC, miR-149-5p mimic, miR-149-5p mimic +pc-NC and miR-149-5p mimic + pc-YWHAZ. (**M** and **N**) Capacities of migration and invasion were analyzed in treated HGC-27 and AGS cells. *P <0.05.

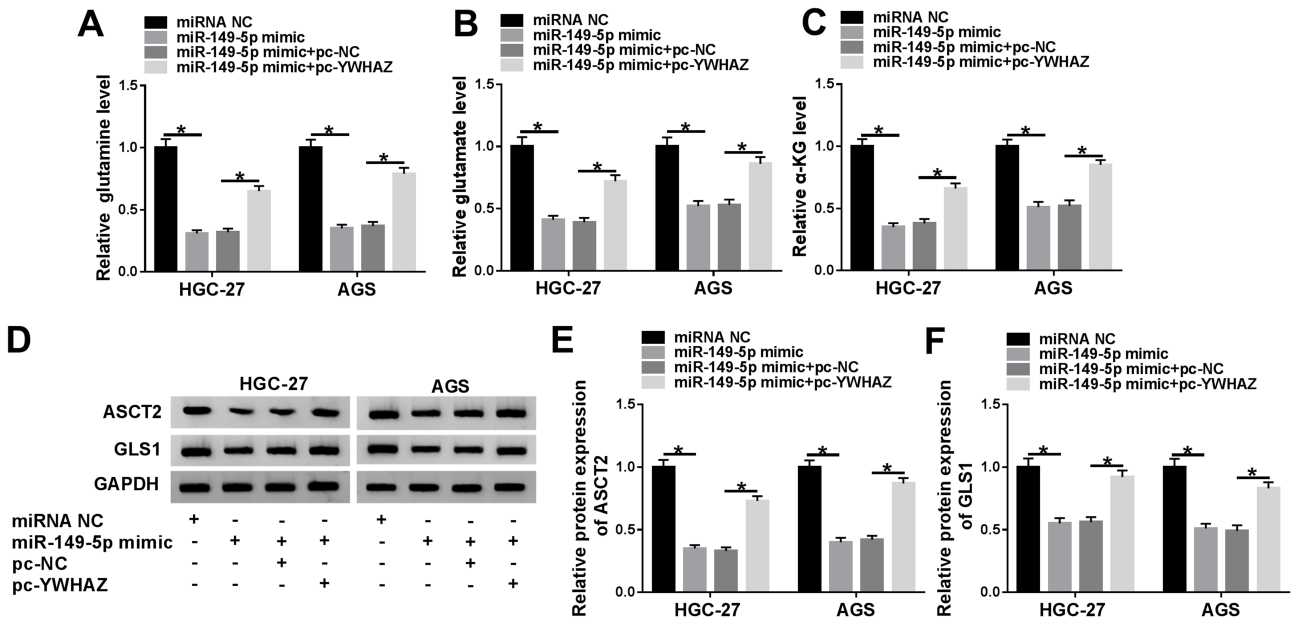

Figure 6 MiR-149-5p-mediated glutaminolysis was overturned through the upregulation of YWHAZ in GC cells. (**A–C**) Expression levels of glutamine, glutamate and α-KG were measured in HGC-27 and AGS cells transfected with miR-NC, miR-149-5p mimic, miR-149-5p mimic +pc-NC and miR-149-5p mimic + pc-YWHAZ. (**D–F**) ASCT2 and GLS1 protein levels were assessed in transfected HGC-27 and AGScells. *P <0.05.

whereas the overexpression of YWHAZ relieved the effect (Figure 7A and B). Meanwhile, the YWHAZ expression level was inversely correlated with the circNHSL1 level in GC tissues (Figure S1). Additionally, miR-149-5p inhibitor could partly the inhibitory action of si-circNHSL1 on YWHAZ expression (Figure 7C and D), further supporting the regulatory of circNHSL1/miR-149-5p/YWHAZ axis in GC cells.

CircNHSL1 Knockdown Repressed GC Cell Growth in vivo

Finally, we established a mice xenograft model of GC to evaluate the impact of circNHSL1 on tumor growth in vivo. Tumor volume and weight were decreased in the presence of circNHSL1 downregulation, verifying that the knockdown of circNHSL1 could restrain GC tumor growth in vivo (Figure 8A and B). Apart from that, we confirmed that the levels of circNHSL1 and YWHAZ were remarkably reduced in tumor tissues from sh-circNHSL1group relative to the sh-NC group (Figure 8C, E, and F), whereas miR-149-5p level was improved in the tumor tissues (Figure 8D). Therefore, it is concluded that circNHSL1 knockdown could dampen GC tumor growth at least partly through the miR-149-5p/YWHAZ axis in vivo.

CircNHSL1 Expression Was Upregulated in Gastric Cancer-Derived Exosomes

Finally, to confirm that exosomes could be isolated from serums, we collected the serums from GC patients and healthy controls. Then, exosomes were isolated from the serums by ultracentrifugation. The extracted exosomes were then examined by a transmission electron microscope and nanoparticle tracking analysis (NTA). As shown in Figure 9A and B, exosomes were typical rounded particles, most of which were 100 nm in diameter. Simultaneously, Western blot analysis proved the presence of serums exosomes marker protein CD63, CD9, and CD81 (Figure 9C). Moreover, to explore the role of circNHSL1 in exosomes, its expression level was detected by RT-qPCR assay. Data suggested that the expression level of circNHSL1 was upregulated in serum exosomes from GC patients (n=20) compared with paired normal controls (Figure 9D). Meanwhile, we verified that the circNHSL1 level was increased in

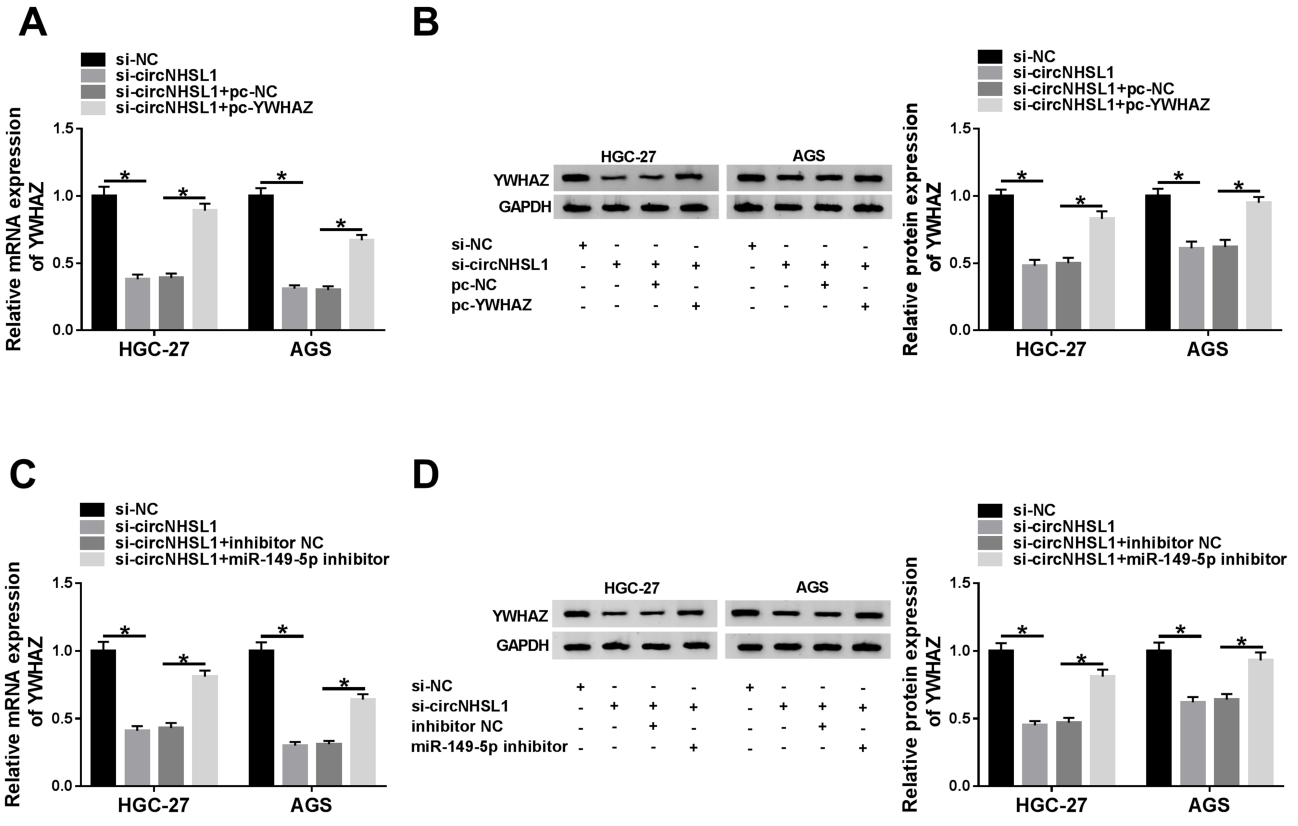

Figure 7 CircNHSL1 regulated YWHAZ expression through sponging miR-149-5p in GC cells. (**A** and **B**) YWHAZ level was detected in HGC-27 and AGS cells transfected with si-NC, si-circNHSL1, si-circNHSL1 + pc-NC and si-circNHSL1 + pc-YWHAZ. (**C** and **D**) YWHAZ level was examined in HGC-27 and AGS cells transfected with si-NC, si-circNHSL1, si-circNHSL1 + inhibitor NC and si-circNHSL1 + miR-149-5p inhibitor. *P <0.05.

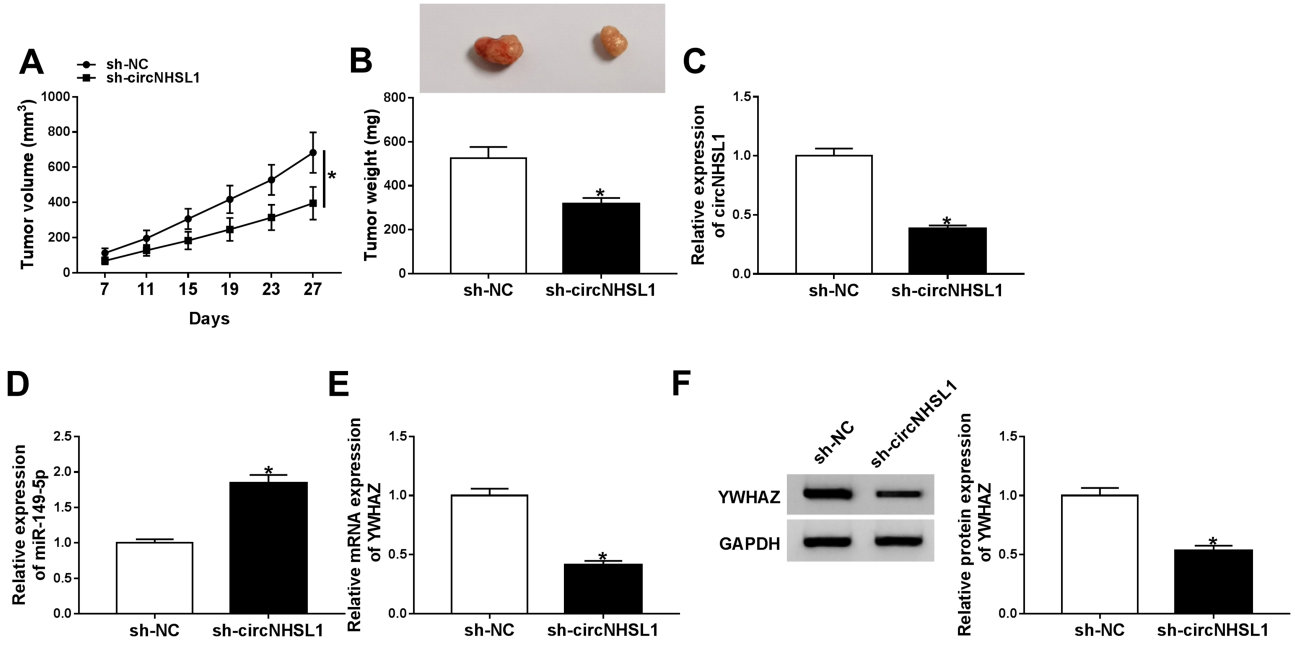

Figure 8 CircNHSL1 deficiency inhibited GC cell growth in vivo. (**A** and **B**) Tumor volume and tumor weight were measured in xenografts. (**C** and **D**) The levels of circNHSL1 and miR-149-5p were detected in by RT-qPCR assay in xenografts. (**E**) YWHAZ mRNA level in xenografts was examined by RT-qPCR. (**F**) YWHAZ protein level in xenografts was measured by Western blot assays. *P <0.05.

circNHSL1 in exosomes from HGC-27 and AGS cells versus GES-1 cells (Figure 9E). Together, these data indicated that the circNHSL1 was highly expressed in GC cell-derived exosomes.

Discussion

In recent years, owing to the rapid development of sequencing technologies, the function and mechanism of circRNAs are increasingly discovered and confirmed.[31,32] Moreover, circRNAs have been reported to be candidate biomarkers for many types of cancer.[33] As the research moves along, an increasing number of circRNAs have been confirmed to be associated with the development and progression of various cancers, including GC.[34] Noteworthily, a recent report has confirmed that circNHSL1 (hsa_circ_0006835) was abnormally increased in GC.[10] However, in the present, there are few reports on the mechanism of circNHSL1 in the regulation of GC. In this manuscript, circNHSL1 was displayed to be upregulated in tissues and cells. Moreover, our data suggested that circNHSL1 could work as an underlying biomarker for prognosis in GC, owing to the stable loop structure and copious cytoplasm. Functionally, circNHSL1 knockdown repressed GC cell migration, invasion, and glutaminolysis, suggesting the pro-cancer effect of circNHSL1, in agreement with the previous report.[10]

Currently, it is widely recognized that circRNAs could serve as a ceRNA of miRNAs to regulate the expression of target miRNAs.[35] In this paper, miR-149-5p was first confirmed to be a direct target of circNHSL1. Moreover, miR-149-5p was proved to be decreased in GC tissues and cells. Intriguingly, miR-149-5p silencing abolished si-circNHSL1-mediated decline in migration, invasion, and glutaminolysis. The inhibitory action of miR-149-5p on GC progression was also testified in the previous literature.[36] As we have known, miRNAs could regulate the development of tumors through targeting mRNAs.[37] Our results first verified that miR-149-5p interacted with YWHAZ and suppressed its expression. Meanwhile, the TCGA database confirmed that YWHAZ was upregulated in GC. Apart from that, our study also demonstrated the high expression of YWHAZ in GC tissues and cells. Thus, we chose YWHAZ for further exploration. Functionally, YWHAZ overexpression reversed the suppressive effect of miR-149-5p on migration, invasion and glutaminolysis. The promotion action of YWHAZ on migration and invasion was proved in breast cancer,[38] cervical cancer,[39] and ovarian cancer.[40] Finally, rescue assays confirmed that miR-149-5p inhibitor mitigated the circNHSL1 knockdown-caused reduction on the YWHAZ level of GC cells in vitro, further supporting that circNHSL1 could act as a ceRNA of miR-149-5p to affect YWHAZ expression.

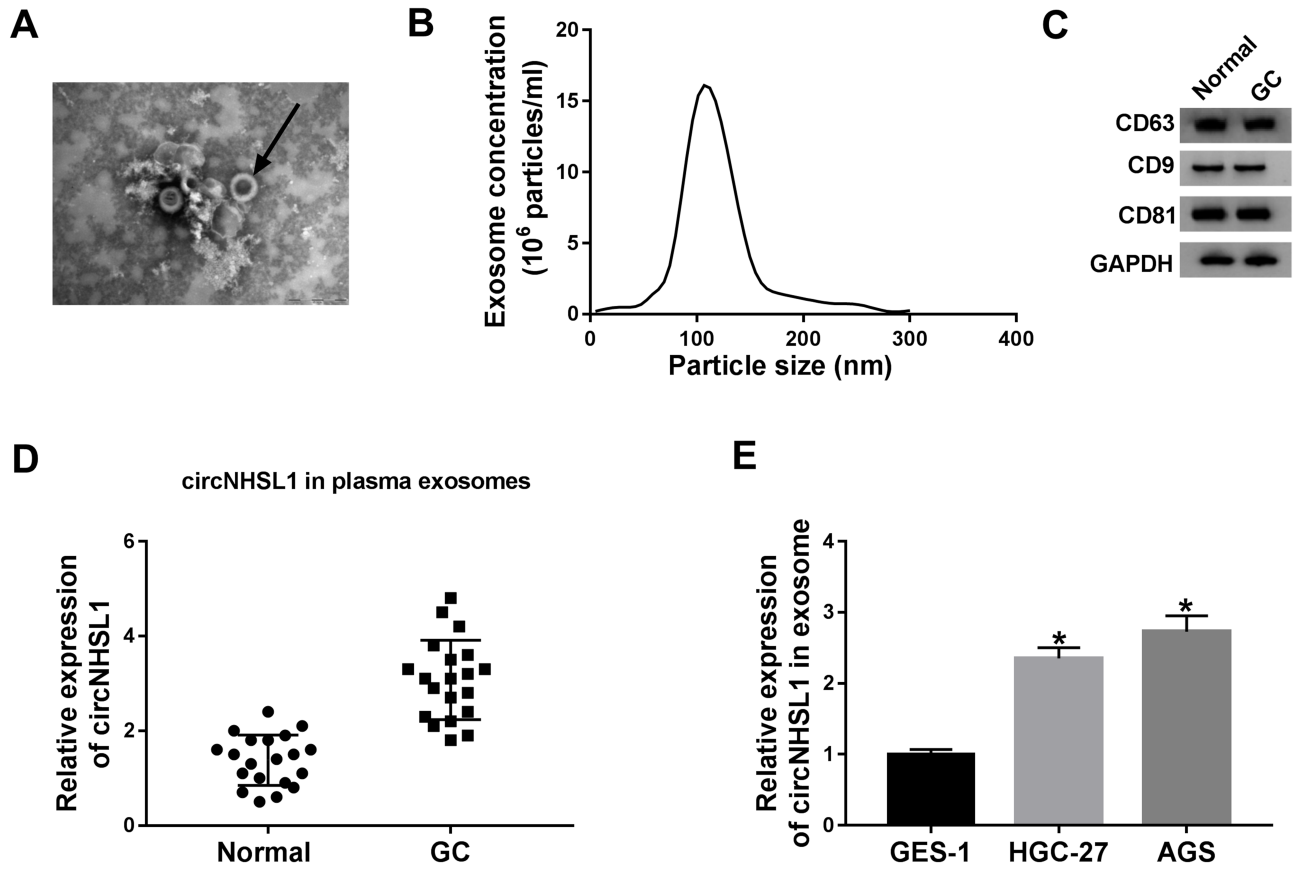

Figure 9 CircNHSL1 was highly expressed in gastric cancer-derived exosomes. (**A**) Transmission electron microscope was applied to detect exosome's morphology. Black arrows indicated the endogenous exosomes. (**B**) Nanoparticle tracking analysis (NTA) determined the distribution of exosome size and concentrations. (**C**) Western blot assay was used to measure the protein levels of CD63, CD9, and CD81 in serum exosomes from GC patients (n=20) and healthy controls (n=20). (**D**) RT-qPCR assay was performed to assess the expression level of circNHSL1 in 20 pairs of GC serum exosomes and paired normal controls. (**E**) The expression level of circNHSL1 was measured in exosomes from GES-1, HGC-27 and AGS cells. *P <0.05.

Additionally, our research also confirmed that circNHSL1 downregulation hindered GC tumor growth by the miR-149-5p/YWHAZ axis in vivo. The innovation of this research is not only that the circRNA-miRNA-mRNA network was constructed by the circNHSL1/miR-149-5p/YWHAZ axis in GC, but also that the progression of GC is related to the glutaminolysis.

Interestingly, circRNAs has been pointed out to be enriched and stable in exosomes.[5] In this study, we found the high expression of circNHSL1 in GC cell-derived exosomes. Hence, we will continue to explore the underlying role and mechanism of exosomalcircNHSL1 in GC progression in the subsequent study.

Conclusion

Taken together, our findings first revealed that circNHSL1 knockdown could retard GC progression in vitro, and GC tumor growth in vivo at least partly through the miR-149-5p/YWHAZ axis. This study revealed that circNHSL1 might be a potential therapeutic target for GC.

Disclosure

The authors report no funding and no conflicts of interest for this work.

References

1. Bray F, Ferlay J, Soerjomataram I, Siegel RL, Torre LA, Jemal A. Global cancer statistics 2018: GLOBOCAN estimates of incidence and mortality worldwide for 36 cancers in 185 countries. *CA Cancer J Clin*. 2018;68(6):394–424. doi:10.3322/caac.21492
2. Coburn N, Cosby R, Klein L, et al. Staging and surgical approaches in gastric cancer: a systematic review. *Cancer Treat Rev*. 2018;63:(104–-115. doi:10.1016/j.ctrv.2017.12.006
3. Lehnert T, Rudek B, Buhl K, Golling M. Surgical therapy for loco-regional recurrence and distant metastasis of gastric cancer. *Eur J Surg Oncol*. 2002;28(4):455–461. doi:10.1053/ejso.2002.1260
4. Qu S, Yang X, Li X, et al. Circular RNA: a new star of noncoding RNAs. *Cancer Lett*. 2015;365(2):141–148. doi:10.1016/j.canlet.2015.06.003

5. Li Y, Zheng Q, Bao C, et al. Circular RNA is enriched and stable in exosomes: a promising biomarker for cancer diagnosis. *Cell Res*. 2015;25(8):981–984. doi:10.1038/cr.2015.82
6. Zhang H, Zhu L, Bai M, et al. ExosomalcircRNA derived from gastric tumor promotes white adipose browning by targeting the miR-133/PRDM16 pathway. *Int J Cancer*. 2019;144 (10):2501–2515. doi:10.1002/ijc.31977
7. Meng S, Zhou H, Feng Z, et al. CircRNA: functions and properties of a novel potential biomarker for cancer. *Mol Cancer*. 2017;16(1):94. doi:10.1186/s12943-017-0663-2
8. Han J, Zhao G, Ma X, et al. CircRNA circ-BANP-mediated miR-503/ LARP1 signaling contributes to lung cancer progression. *Biochim Biophys Res Commun*. 2018;503(4):2429–2435. doi:10.1016/j.bbrc.2018.06.172
9. Zhu Q, Lu G, Luo Z, et al. CircRNA circ_0067934 promotes tumor growth and metastasis in hepatocellular carcinoma through regulation of miR-1324/FZD5/Wnt/beta-catenin axis. *Biochim Biophys Res Commun*. 2018;497(2):626–632. doi:10.1016/j.bbrc.2018.02.119
10. Zhu Z, Rong Z, Luo Z, et al. Circular RNA circNHSL1 promotes gastric cancer progression through the miR-1306-3p/SIX1/vimentin axis. *Mol Cancer*. 2019;18(1):126. doi:10.1186/s12943-019-1054-7
11. Bartel DP. MicroRNAs: genomics, biogenesis, mechanism, and function. *Cell*. 2004;116(2):281–297. doi:10.1016/s0092-8674(04)00045-5
12. Ueda T, Volinia S, Okumura H, et al. Relation between microRNA expression and progression and prognosis of gastric cancer: a microRNA expression analysis. *Lancet Oncol*. 2010;11 (2):136–146. doi:10.1016/s1470-2045(09)70343-2
13. Ye X, Chen X. miR-149-5p inhibits cell proliferation and invasion through targeting GIT1 in medullary thyroid carcinoma. *Oncol Lett*. 2019;17(1):372–378. doi:10.3892/ol.2018.9628
14. Shao S, Wang C, Wang S, Zhang H, Zhang Y. Hsa_circ_0075341 is up-regulated and exerts oncogenic properties by sponging miR-149-5p in cervical cancer. *Biomed Pharmacother*. 2019;121:109582. doi:10.1016/j.biopha.2019.109582
15. Kong YG, Cui M, Chen SM, Xu Y, Xu Y, Tao ZZ. LncRNA-LINC00460 facilitates nasopharyngeal carcinoma tumorigenesis through sponging miR-149-5p to up-regulate IL6. *Gene*. 2018;639:77–84. doi:10.1016/j.gene.2017.10.006
16. Luo X, Wang GH, Bian ZL, et al. Long non-coding RNA CCAL/ miR-149/FOXM1 axis promotes metastasis in gastric cancer. *Cell Death Dis*. 2018;9(10):993. doi:10.1038/s41419-018-0969-z
17. Wang Y, Zheng X, Zhang Z, et al. MicroRNA-149 inhibits proliferation and cell cycle progression through the targeting of ZBTB2 in human gastric cancer. *PLoS One*. 2012;7(10):e41693. doi:10.1371/journal.pone.0041693
18. Shi X, Wang X, Hua Y. LncRNA GACAT1 promotes gastric cancer cell growth, invasion and migration by regulating MiR-149-mediated OF ZBTB2 And SP1. *J Cancer*. 2018;9(20):3715–3722. doi:10.7150/jca.27546
19. Goossens K, Van Poucke M, Van Soom A, Vandesompele J, Van Zeveren A, Peelman LJ. Selection of reference genes for quantitative real-time PCR in bovine preimplantation embryos. *BMC Dev Biol*. 2005;5:27. doi:10.1186/1471-213x-5-27
20. Mao L, Zhang Y, Deng X, Mo W, Yu Y, Lu H. Transcription factor KLF4 regulates microRNA-544 that targets YWHAZ in cervical cancer. *Am J Cancer Res*. 2015;5(6):1939–1953.
21. Li Y, Wang J, Dai X, et al. miR-451 regulates FoxO3 nuclear accumulation through Ywhaz in human colorectal cancer. *Am J Transl Res*. 2015;7(12):2775–2785.
22. Chi J, Liu T, Shi C, et al. Long non-coding RNA LUCAT1 promotes proliferation and invasion in gastric cancer by regulating miR-134-5p/YWHAZ axis. *Biomed Pharmacother*. 2019;118:109201. doi:10.1016/j.biopha.2019.109201
23. Guo F, Gao Y, Sui G, et al. miR-375-3p/YWHAZ/beta-catenin axis regulates migration, invasion, EMT in gastric cancer cells. 2019;46 (2):144–152. doi:10.1111/1440-1681.13047
24. Puch-Hau C, Sanchez-Tapia IA, Patino-Suarez V, et al. Evaluation of two independent protocols for the extraction of DNA and RNA from different tissues of sea cucumber Isostichopusbadionotus. *MethodsX*. 2019;6:1627–1634. doi:10.1016/j.mex.2019.07.010
25. Livak KJ, Schmittgen TD. Analysis of relative gene expression data using real-time quantitative PCR and the 2(-Delta Delta C(T)) Method. *Methods*. 2001;25(4):402–408. doi:10.1006/meth.2001.1262
26. Guo X, Qiu W, Liu Q, et al. Immunosuppressive effects of hypoxia-induced glioma exosomes through myeloid-derived suppressor cells via the miR-10a/Rora and miR-21/Pten Pathways. *Oncogene*. 2018;37(31):4239–4259. doi:10.1038/s41388-018-0261-9
27. Yang L, Venneti S, Nagrath D. Glutaminolysis: a hallmark of cancer metabolism. *Annu Rev Biomed Eng*. 2017;19:163–194. doi:10.1146/annurev-bioeng-071516-044546
28. van Geldermalsen M, Wang Q, Nagarajah R, et al. ASCT2/SLC1A5 controls glutamine uptake and tumour growth in triple-negative basal-like breast cancer. *Oncogene*. 2016;35(24):3201–3208. doi:10.1038/onc.2015.381
29. Jin L, Alesi GN, Kang S. Glutaminolysis as a target for cancer therapy. *Oncogene*. 2016;35(28):3619–3625. doi:10.1038/onc.2015.447
30. Militello G, Weirick T, John D, Doring C, Dimmeler S, Uchida S. Screening and validation of lncRNAs and circRNAs as miRNA sponges. *Brief Bioinform*. 2017;18(5):780–788. doi:10.1093/bib/bbw053
31. Gao D, Qi X, Zhang X, Fang K, Guo Z, Li L. hsa_circRNA_0006528 as a competing endogenous RNA promotes human breast cancer progression by sponging miR-7-5p and activating the MAPK/ERK signaling pathway. 2019;58(4):554–564. doi:10.1002/mc.22950
32. Xu L, Feng X, Hao X, et al. CircSETD3 (Hsa_circ_0000567) acts as a sponge for microRNA-421 inhibiting hepatocellular carcinoma growth. *J Exp Clin Cancer Res*. 2019;38(1):98. doi:10.1186/s13046-019-1041-2
33. Zaporozhchenko IA, Ponomaryova AA, Rykova EY, Laktionov PP. The potential of circulating cell-free RNA as a cancer biomarker: challenges and opportunities. *Expert Rev Mol Diagn*. 2018;18 (2):133–145. doi:10.1080/14737159.2018.1425143
34. Fang X, Wen J, Sun M, Yuan Y, Xu Q. CircRNAs and its relationship with gastric cancer. *J Cancer*. 2019;10(24):6105–6113. doi:10.7150/jca.32927
35. Kulcheski FR, Christoff AP, Margis R. Circular RNAs are miRNA sponges and can be used as a new class of biomarker. *J Biotechnol*. 2016;238:42–51. doi:10.1016/j.jbiotec.2016.09.011
36. Zhang X, Wang S, Wang H, et al. Circular RNA circNRIP1 acts as a microRNA-149-5p sponge to promote gastric cancer progression via the AKT1/mTOR pathway. 2019;18(1):20. doi:10.1186/s12943-018-0935-5
37. Reddy KB. MicroRNA (miRNA) in cancer. *Cancer Cell Int*. 2015;15 (1):38. doi:10.1186/s12935-015-0185-1
38. Wang W, Zhang L, Wang Y, et al. Involvement of miR-451 in resistance to paclitaxel by regulating YWHAZ in breast cancer. *Cell Death Dis*. 2017;8(10):e3071. doi:10.1038/cddis.2017.460
39. Ji N, Wang Y, Bao G, Yan J, Ji S. LncRNA SNHG14 promotes the progression of cervical cancer by regulating miR-206/YWHAZ. *Pathol Res Pract*. 2019;215(4):668–675. doi:10.1016/j.prp.2018.12.026
40. Yang B, Sun L, Liang L. MiRNA-802 suppresses proliferation and migration of epithelial ovarian cancer cells by targeting YWHAZ. *J Ovarian Res*. 2019;12(1):100. doi:10.1186/s13048-019-0576-3